

Energy Based Analysis of Laser Microchanneling Process on Polymethyl Methacrylate (PMMA)

Shashi Prakash and Subrata Kumar

Abstract CO₂ laser micromachining provides low cost machining solution for fabrication of three dimensional microfluidic channels on poly-methyl-methacrylate (PMMA). In this research work CO₂ laser microchanneling process has been analyzed from the first principle. Considering the Gaussian distribution of laser beam, an energy based model has been proposed to predict the microchannel depth and channel profile. For fabricating microfluidic devices, PMMA has emerged as a cheap alternative to many other costly materials like silicon, quartz etc. Its material properties like absorptivity and thermal properties have been investigated. In order to physically verify the proposed model, experiments have been performed on a 3 mm thick PMMA sheet and actual and predicted results have been compared. Simultaneous TGA/DSC tests have been conducted to determine various thermal properties of PMMA. Since thermal conductivity of the PMMA is very low, the conduction loss has been neglected while developing the model. The proposed model successfully predicts the channel depth and profile without much loss of accuracy. energy based analysis has been found to be simple yet powerful method to predict the channel dimensions for low thermal conductivity materials.

Keywords CO₂ laser beam machining · PMMA · Microchanneling · Energy analysis

1 Introduction

The use of lasers in micro manufacturing is growing rapidly. The usual advantages of using laser in micromachining are its simplicity in operation and fast production rate. CO₂ laser machining is a noncontact and heat based material removal process

S. Prakash (✉) · S. Kumar
Mechanical Engineering Department, Indian Institute of Technology Patna, Patna, India
e-mail: spasthan@iitp.ac.in

S. Kumar
e-mail: subrata@iitp.ac.in

where lower surface roughness and higher dimensional tolerance can be achieved using low beam diameter and highly concentrated beam energy (Madic et al. 2012). Laser micro-machining is a material processing technique that employs lasers to induce managed vaporization to provide required micro scale geometrical shape and dimensional ablation. Despite the facts that laser machining is a technically complicated process, research work has allowed the fabrication of precise, smooth and clean components at high speed. Lasers do not employ traditional tool-fixture setups, which makes the whole process lot easier as well as less time consuming. With different wavelength ranges of available laser systems, one can possibly machine all kinds of materials. Moreover, apart from cutting, lasers can also do many other jobs like welding, drilling and forming. Owing to this, modern industries are now replacing the conventional machines with laser machining system. This also results in getting lower cost, much higher productivity and better surface quality (Zhou et al. 2004).

Miniaturization of analytical tools and devices has been an ongoing trend to improve the performance of analytical tools. Microdevices make many different types of analysis including chromatography, electrophoresis and DNA analysis possible. Such microdevices reduce sample consumption, cost, time to results and also yield better performance and portability. Microchannels are part of several microfluidic devices, microelectronics based devices and micro-electro-mechanical systems (MEMS). Microchannels are used in various bio-analytical devices, DNA synthesis, electrophoresis etc. The size specifications of these microchannels vary in different types of applications. Microchannels are generally defined as channels having any of the sizes in micron range (1–999 μm). Microchannels are generally fabricated with non-conventional manufacturing techniques unlike channels of higher size which can be fabricated using conventional fabrication techniques. Microchannels with high aspect ratios are used in most of the devices (Costano-Alvarez et al. 2008). However, microchannels with low aspect ratios are also used in several applications like particle separation devices, DNA analysis etc. (Russom et al. 2009).

In earlier times, silicon, glass and quartz have been the most preferred materials for microfluidic devices because of some of the favorable properties like optical transparency, high mechanical strength, high melting point, and well defined surface characteristics. However, producing such devices on these substrates has always been a costly affair. Producing microchannels on such substrates involve typically longer manufacturing processes like lithography, embossing and etching (Iliescu et al. 2012). The use of polymeric materials for microfluidic devices is a recent trend. Polymers offer several advantages over other materials in terms of lower cost, lighter weight and easier manufacturing. Thus they can be made portable and disposable (Qi et al. 2009).

In recent times, poly-methyl-methacrylate (PMMA) has been evolved as one of the most preferred polymer for many microfluidic devices (Prakash et al. 2014). PMMA possesses high absorbance in mid-infrared zone which makes it particularly suitable for CO_2 laser (Malek 2006). It has low heat capacity and low heat conduction. Therefore, all the energy transferred to material is utilized in rapid

vaporization (Prakash et al. 2013). PMMA also offers high degree of optical transparency which makes it perfectly suitable for many microfluidic devices. PMMA has been especially useful in applications where high temperature is not involved because of its low thermal stability.

CO₂ laser ablation has been investigated by various authors over the years. Helebrant et al. (1993) developed one dimensional steady state heat conduction equation for CO₂ laser irradiation of glass. Julia et al. (1998) utilized the energy balance method for CO₂ laser ablation of biological tissues. They have also considered the effects of temperature on optical properties. Laser micromachining of PMMA has also been studied by Klank et al. (2002). They utilized the CO₂ laser for rapid fabrication of microfluidic structures on PMMA Snakenborg et al. (2004) analyzed the laser micro-machining process on PMMA using 1-dimensional heat conduction equation. Xiang et al. (2006) used the three dimensional transient heat conduction equations to model the CO₂ laser cutting of PMMA. They used finite element method to solve the model. Yuan and Das (2007) developed analytical model for low power CO₂ laser ablation of PMMA. The model included heat conduction as well as energy loss in decomposition of PMMA. Shulepov et al. (2010) proposed a thermo-chemical model for CO₂ laser ablation of PMMA and polyimide. They studied the phenomenon of plasma generation with CO₂ laser irradiation. The model considers the plasma screening effect. They observed the presence of plasma pipe in CO₂ laser cutting at high intensities. However, most of the models employ computer simulation based numerical analysis to determine the channel profile and depth.

In this research work, CO₂ laser based microchanneling process has been analyzed based on simple energy balance method. Energy based modeling also gives physical insight into the laser micromachining process. Channel profile and depth have been determined utilizing this model. Implementation of finite element analysis or other numerical analysis based modeling is difficult as well as time consuming when compared to energy based modeling. This energy based model is simple in nature and can readily be applied in laser micromachining processes without much loss of accuracy for most of the polymers. This energy based modeling is especially suitable for materials having very low thermal conductivity.

2 Determination of Material Properties

PMMA is one of the most widely used amorphous thermoplastic materials. Because of its high optical transparency it is widely used in place of glass. It is also known by many other names like Plexiglass, Lucite, Perspex and Acrylite. PMMA is generally produced by polymerization process. Most of the properties of PMMA vary product to product because of large numbers of commercial compositions which are copolymers with co-monomers other than methyl methacrylate. The chemical structure of PMMA has been given in Fig. 1.

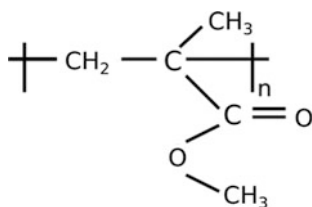


Fig. 1 Chemical structure of poly-methyl-methacrylate (PMMA)

PMMA behaves differently with different kinds of lasers according to their wavelength. Transparent PMMA generally transmits a major part of laser beam of near IR wavelength (1.06 μm). However, it shows a good absorption in ultraviolet and mid infrared range (10.6 μm). In order to determine the absorptivity of used PMMA specimen for CO₂ laser wavelength i.e. 10.6 μm , far-infrared (FIR) spectroscopic analysis has been performed using Shimadzu IRAffinity-1 spectrophotometry.

In this test light beams covering infrared spectrum are produced. These are based on the fact that the molecules of particular substance absorb specific frequencies. Two separate tests for determining absorptivity and reflectivity have been performed. The experiments have been performed under normal atmospheric conditions. These tests give the absorptivity and reflectivity values of used PMMA over a wide range of wavelengths. In this experiment cast acrylic (PMMA) of 3 mm thickness has been used. The transmissivity and reflectivity results are shown in Fig. 2. The reflectivity and transmissivity corresponding to 10.6 μm i.e. 943 cm^{-1} have been found to be 4.67 and 0.31 % respectively. Therefore it can be concluded that the used PMMA specimen absorbs nearly 95 % of CO₂ laser radiation. In other words, it can be assumed that 95 % of total CO₂ laser power is utilized in material processing, while remaining 5 % is lost. This amount is still very high when compared to laser interactions with many other materials. Therefore, with very little

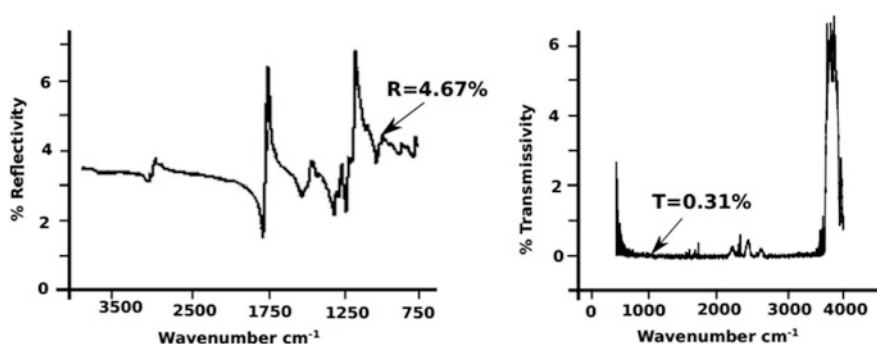


Fig. 2 Reflectivity and transmissivity test of PMMA

loss of total beam power, CO₂ laser can be assumed to be perfectly suitable for PMMA.

Determination of thermal properties is most important for understanding of CO₂ laser interaction of PMMA. In order to determine its various thermal properties, Simultaneous Thermogravimetric analysis/Differential scanning calorimetry (TGA/DSC) test have been performed. The tests have been performed using STA 6000 (Perkin-Elmer).

Table 1 lists the thermal properties obtained using TGA/DSC tests. The heating of the sample has been performed at temperature increment rate of 10 °C per minute. An initial weight of 32 mg of the sample has been taken. TGA test reveals the thermal decomposition behavior of PMMA. TGA curve has been shown in Fig. 3 in black dashed line. PMMA starts turning into rubbery state at 110 °C. It starts melting at around 160 °C. However, both the processes do not involve significant latent heat. Sample starts vaporizing at 220 °C. At 377 °C, the highest rate of decomposition takes place. The sample gets completely vaporized at 393 °C. DSC curve has been shown in red in color. Area under the DSC curve represents the enthalpy of vaporization process. Some of the material properties have been taken from the available literature and been mentioned in this table. In this modeling, it has been assumed that material properties do not change with temperature.

In this research work, commercial CO₂ laser, (VLS 3.60, Universal Laser System Inc., USA), has been used (Fig. 4). The laser is quasi-continuous (QCW) wave in nature. The system is air-cooled and no other cooling aid has been used during the experiments. Laser head can move in X and Y direction while bed moves in Z-direction. The system is fully CNC controlled and runs through graphics based software like AutoCAD, Corel draw etc. The focal length of the focusing lens is 50 mm. Further details of CO₂ laser system has been provided in Table 2. The pulse frequency of this system can be varied by adjusting the speed and PPI (pulse per inch) parameter. The output power of the laser system remains constant over the time during “ON” period. Figure 5 shows the power time variation of the laser system. Laser beam can be focused to a very thin spot. Laser beam diameter has been determined on a 1 mm thick PMMA sheet as described by Powell (1998).

Table 1 Thermal properties obtained from simultaneous TGA/DSC

Property	Symbol	Value
Glass transition temperature	T _g	110 °C
Melting temperature	T _m	165 °C
Thermal decomposition starts at	T _{ds}	230 °C
Thermal decomposition ends at	T _{de}	393 °C
Specific heat	c _p	1.466 kJ/kg-K
Enthalpy of vaporisation	ΔH _v	2757 kJ/kg
Material density (Radice et al. 2012)	ρ	1070 kg/m ³
Thermal conductivity (Radice et al. 2012)	k	0.19 W/mK

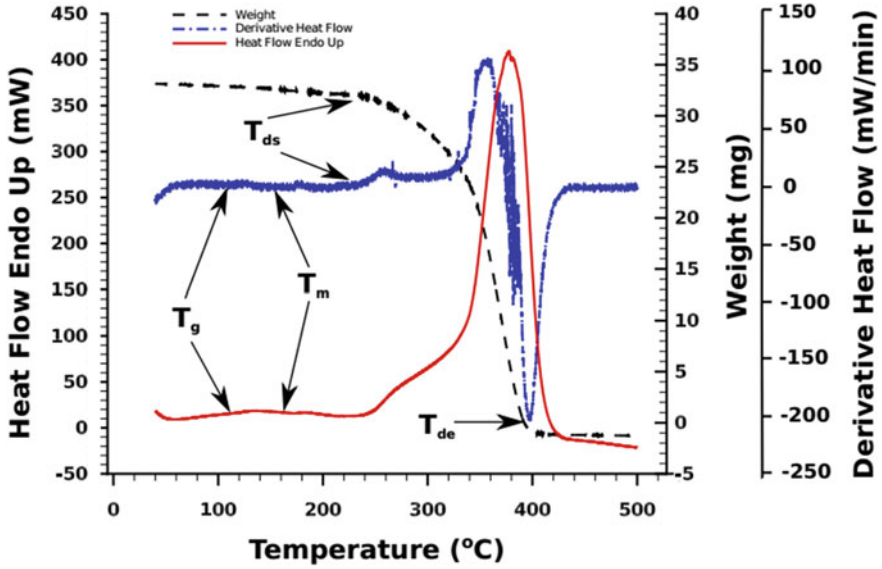


Fig. 3 Simultaneous TGA/DSC test results of PMMA

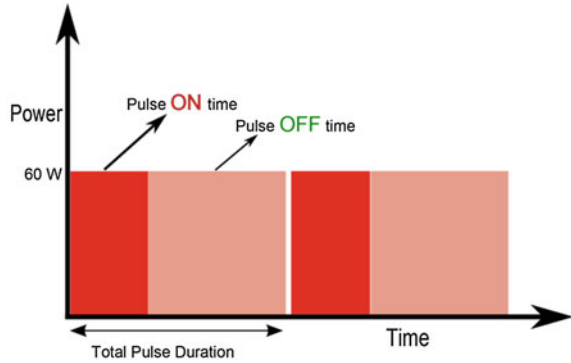
Fig. 4 Universal CO₂ laser systems



Table 2 CO₂ Laser system specification

Class type	IV
Max power	60 W
Wavelength	10.6 μm
Output beam shape	Gaussian
M ² value	<1.5
Mode of operation	RF excited ON/OFF
Maximum working area	24" × 12"

Fig. 5 Power-time variations for CO₂ laser



Average beam diameter has been found to be 237 μm . Also, beam periphery has been found to be very closely approximating the circle. Laser system can be allowed to work in two different modes namely raster mode and vector mode. In this work, all experiments have been performed in vector cutting mode of the laser system. All the experiments have been performed at focus point of the lens resulting in minimum beam spot diameter.

3 Energy Based Modeling of CO₂ Laser Microchanneling of PMMA

The thermal conductivity of PMMA is very low. As such the energy loss due to thermal conduction is also very small. Therefore, neglecting the conduction heat loss does not affect the modeling process to a significant extent. Also the heated zone is extremely small in a microchanneling process. The maximum temperature rise is also not significantly high. These factors make the convection and radiation loss to be negligible. Material properties inevitably change with temperature. However, since the vaporization temperature of the PMMA is small, these changes may also be assumed to be insignificant for making the modeling simpler and easy to understand. As the laser beam vaporizes the material, in the way they also interact with the vaporizing particles. Some part of the incoming beam energy gets absorbed by such particles. However, since the amount of vaporizing material is very small, the energy absorption in this process can also be assumed to be very small. Therefore, on the basis of the above discussion, following assumptions have been made in this energy based modeling;

1. There is no conduction heat loss into the substrate.
2. There is no convection and radiation loss.
3. The material properties do not change and remains constant throughout the process.

Let the laser beam moves through the center line in x-direction and at the center line $y = 0$. Figure 6 shows the schematic diagram of laser beam movement on PMMA. Since the beam is near perfect Gaussian, the cross-section of the produced microchannel is also nearly Gaussian.

The optical intensity of a Gaussian laser beam at any location (x, y) can be given by following Eq. (1) (Dahotre and Harimkar 2007):

$$I(x, y) = I_0 e^{-2\left(\frac{x^2+y^2}{w^2}\right)} \quad (1)$$

where,

I = laser beam intensity at (x, y) ,

I_0 = laser beam peak intensity = $\frac{2P}{\pi w^2}$;

P is average laser power

w = beam spot radius.

Let us consider an infinitesimally small area $dA = dx \times dy$ within the beam diameter (Fig. 6). P is the average laser power supplied for the time dt . Let α is the absorptivity of the material for CO₂ laser beam wavelength. The laser beam travels with a scanning speed U (Fig. 7).

Since the conduction and radiation energy losses are negligible and PMMA quickly vaporizes without undergoing significant melting, it can be assumed that all the energy given by laser to PMMA is utilized into material removal.

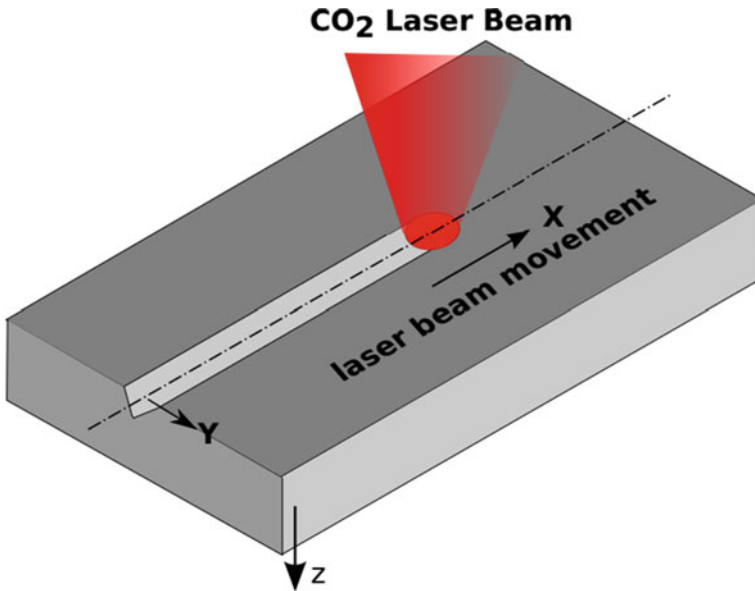


Fig. 6 Schematic of laser microchanneling process on PMMA

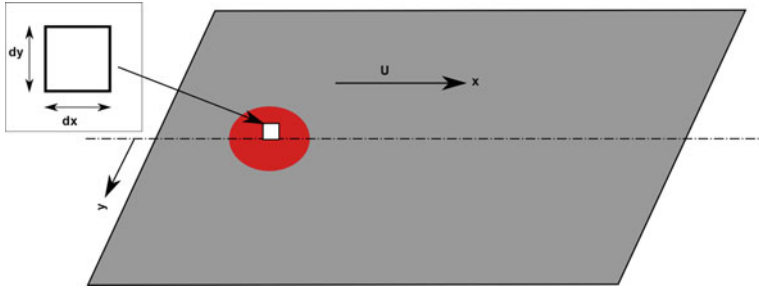


Fig. 7 Focused laser beam moving in x-direction

Energy transfer from laser to the small area dA can be computed as follows:
 Amount of laser energy transferred to area dA ;

$$E_{\text{laser}} = \alpha \times I_0 e^{-2\left(\frac{x^2+y^2}{w^2}\right)} \times dA \times dt = \alpha \times I_0 e^{-2\left(\frac{x^2+y^2}{w^2}\right)} \times dA \times \frac{dx}{U} \quad (2)$$

Energy required to vaporize the small volume can be computed as per Eq. (3):

$$E_{\text{vaporization}} = m(c_p \Delta T + H_L) = \rho \times dA \times dz (c_p \Delta T + H_L) \quad (3)$$

where,

m = Mass of the vaporized volume,

ρ = mass density of PMMA

dz = depth of vaporized volume

ΔT = Temperature change (from room temperature to vaporization temperature),

H_L = Latent heat of vaporization

Equating Eqs. (2) and (3),

$$E_{\text{laser}} = E_{\text{vaporization}}$$

$$\alpha \times I_0 e^{-2\left(\frac{x^2+y^2}{w^2}\right)} \times dA \times \frac{dx}{U} = \rho \times dA \times dz (c_p \Delta T + H_L)$$

$$dz = \alpha \times I_0 e^{-2\left(\frac{x^2+y^2}{w^2}\right)} \times \frac{dx}{U} \times \frac{1}{\rho(c_p \Delta T + H_L)}$$

Applying the limits;

$$\int_0^Z dz = \int_{-\infty}^{+\infty} I_0 e^{-2\left(\frac{x^2+y^2}{w^2}\right)} \times \frac{dx}{U} \times \frac{\alpha}{\rho(c_p \Delta T + H_L)}$$

$$Z = \frac{\alpha\sqrt{2}}{w\rho\sqrt{\pi}(c_p\Delta T + H_L)} \times e^{-2\left(\frac{y^2}{w^2}\right)} \times \frac{P}{U} \quad (4)$$

At the centerline i.e. at $y = 0$, $Z = Z_{\max}$

$$Z_{\max} = \frac{\alpha\sqrt{2}}{w\rho\sqrt{\pi}(c_p\Delta T + H_L)} \times \frac{P}{U} \quad (5)$$

$$Z = Z_{\max}e^{-2\left(\frac{y^2}{w^2}\right)} \quad (6)$$

Equation (5) can be used to determine the maximum depth of the microchannel, i.e. depth at the center. From Eq. (5) it can be interpreted that maximum depth is directly proportional to the laser input power. However, the maximum channel depth decreases when scanning speed increases. The channel depth along the radius i.e. along the y axis can be determined by using Eq. (6).

In order to physically verify the developed model experiments have been performed with three distinct levels of power and scanning speed. Average power and scanning speed have been varied at three different levels. Total nine experiments have been performed based on full factorial design as depicted in Table 3. The output characteristics i.e. microchannel depth has been measured using 3-D Olympus microscope. The depth at the center of the microchannel has been termed as microchannel depth. V-Shape of the microchannel has been obtained due to Gaussian nature of laser beam. Figure 8 shows the output characteristics of the produced microchannels.

The ends have been ultrasonically cleaned and polished before measurement. The depth has been found to be consistent across the length of the microchannel. Bulging at the top corners of the microchannels are also visible in Fig. 8. It has also been observed that larger is the energy density, larger is the amount of bulging and splashing due to larger amount of resolidification. Top view of the microchannels reveals that the channels are straight and clean. Some part of the channel

Table 3 Input and output parameters of CO₂ microchanneling process on PMMA

Experiment no.	Power (P)	Scanning speed (U)	Kerf width	Maximum depth
1	2	7.5	255.86	582.12
2	3	7.5	271.21	850
3	4	5	301.91	1553.19
4	3	5	287.84	1233.79
5	3	10	259.7	678.03
6	2	5	273.77	847.43
7	2	10	237.95	471.37
8	4	7.5	276.33	1063.79
9	4	10	267.37	855.15

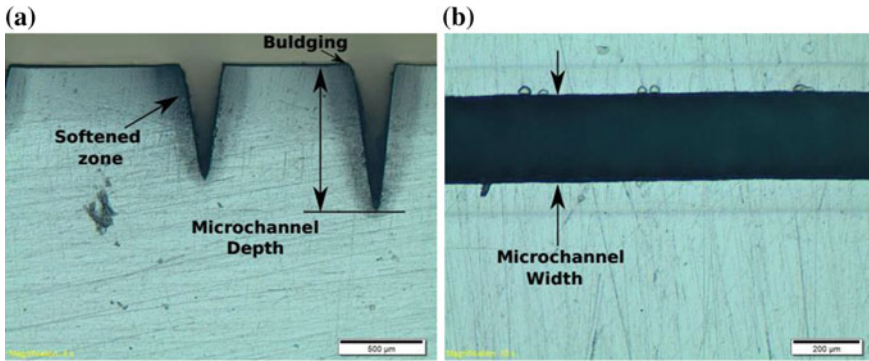


Fig. 8 a Cross-sectional view. b Top view of fabricated microchannel

surrounding becomes softer than the rest of the part after the microchanneling process and therefore has been termed as softened zone. The softened zone can be distinguished by a different color on the optical micrograph image as shown in Fig. 8. The softened zone can also be termed as heat affected zone (HAZ) in this context. The largest width of the softened zone takes place at the top most surface and reduces thereafter. This can be attributed to the fact that heat radiates radially after striking the PMMA surface. Since, highest amount of energy strikes the top-most surface, and reduces thereafter, the largest width of HAZ takes place at the top most surface. No burrs and charring phenomenon has been observed around the microchannels in this process. All the microchannels have been found to be clean and straight. The experiments have been performed on transparent 3 mm thick PMMA sheet.

The depth and profile of the microchannels have also been evaluated based on Eqs. (5) and (6). Table 4 enlists the comparison between actual values and calculated values. Percentage error in prediction of maximum depth has been calculated using following equation.

Table 4 Percentage error calculation

Experiment no.	Experimental depth value	Predicted depth	Error (%)
1	582.12	578.1333	0.68485
2	850	867.2	2.02352
3	1553.19	1734.4	11.6669
4	1233.79	1300.8	5.43123
5	678.03	650.4	4.07504
6	847.43	867.2	2.33293
7	471.37	433.6	8.01281
8	1063.79	1156.267	8.69313
9	855.15	867.2	1.40911

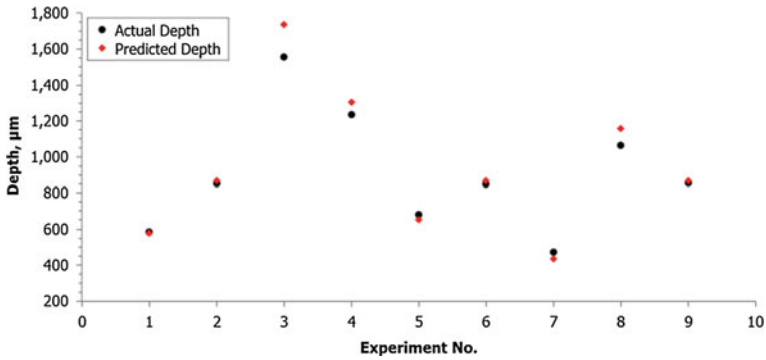


Fig. 9 Graph showing relative errors in actual and predicted values

$$\text{Error} = \left| \frac{\text{Experimental result} - \text{Predicted result}}{\text{Experimental result}} \right| \times 100\%$$

Figure 9 shows the relative differences in actual and predicted values of microchannel depth for all the experiments.

4 Material Removal Mechanism

CO₂ laser ablation is purely thermal ablation in which material removal takes place purely due to vaporization through melting. PMMA strongly absorbs the CO₂ laser and vaporizes immediately as soon as the average laser power crosses certain threshold value. Glass transition temperature of the PMMA has been found to be 110 °C. As soon as temperature of the substrate material reaches to 110 °C, the material starts to turn into glassy rubbery state. Once the temperature of the part crosses glass transition temperature, it may not return to its original condition. The refractivity and some of the surface properties change. The swelling at the surface can be found in the region close to microchannel. This particular region where temperature crossed the glass transition temperature but did not reach to decomposition temperature is termed as softened zone. Since the thermal conductivity of the PMMA is very low, heat gets accumulated into very small region near to microchannel. The formation of softened zone or heat affected zone can be attributed to its low thermal conductivity. Lower conductivity causes localized accumulation of heat in this zone. PMMA involves very little amount of melting at around 160 °C. However, melting does not involve significant amount of latent heat. Therefore, material removal process can be assumed to involve direct sublimation of solid PMMA into vapors without melting. Due to this direct phase change process, the chemical degradation is at minimum. Therefore microchannel edges are of superior quality than many other cutting processes. It has also been observed

during simultaneous TGA/DSC test of PMMA sample. As the temperature of the PMMA reaches to 230 °C, the decomposition of PMMA starts. Although decomposition temperature of the PMMA is not sharp, it takes place very rapidly. PMMA fully decomposes at 393 °C. The highest rate of decomposition takes place at 377 °C. Under the incident laser beam, the temperature of the surface immediately rises to its vaporization temperature and PMMA $(C_5O_2H_8)_n$ decomposes into monomer MMA (methyl-meth-acrylate) units, carbon dioxides (CO_2), carbon monoxides (CO) and water (H_2O)₁₀. The unzipping of various chemical chains leads to formation of monomers. For a radically polymerized PMMA, following two kinds of processes have been proposed. In the first one, the depolymerization process starts with the vinyl end groups. While the second depolymerization process is initiated at saturated C–C bonds. Monomers are highly volatile in nature. Therefore, very little amount of melting takes place. This is one of the reasons that CO_2 laser ablation of PMMA does not involve redeposition of materials. The cut is very much clean with very little or no defects. However a little charring and burning effects are quite visible at the edges forming the bulging zone. The only undesirable effect is softened zone and bulging of the material at the adjacent surfaces. All the byproducts are perfectly volatile in nature and do not cause any further reaction on the PMMA substrate, leaving behind a clean structure. Due to presence of carbon content, a little amount of charring takes place at the edges. The cross sectional shape of the microchannels is of near Gaussian shape. The Gaussian shape occurs due to the Gaussian nature of the laser beam. The microchannels with lower depths follow Gaussian nature more closely than channels with larger depths. However, in most of the cases the cross-section very much resembles to alphabet “V”. This shape of the microchannel also signifies the shape of the beam. Therefore it can be concluded that laser beam shape resembles to the shape of a cone with a pointed crest. The top view of the microchannel is a clean channel structure. Both edges are perfectly parallel to each other.

5 Results and Discussion

All of the experiments have been performed in order to have a wide range of different aspect ratios. The aspect ratio varies from 2 to 5 approximately. Developed model has been tested on all these wide ranges of aspect ratio. The model has been successfully able to predict the maximum depth and profile of the microchannels as shown in Fig. 10 (not to scale). Figure 10 shows the relative differences in actual channel profile and predicted channel profiles. The predicted channel profiles have been drawn with the help of MATLAB software. The background figure in grey shows the actual channel width while the white colored curve shows the predicted channel profile. The minimum error in predicting the maximum depth is 0.68 % while the maximum error is around 11.66 %.

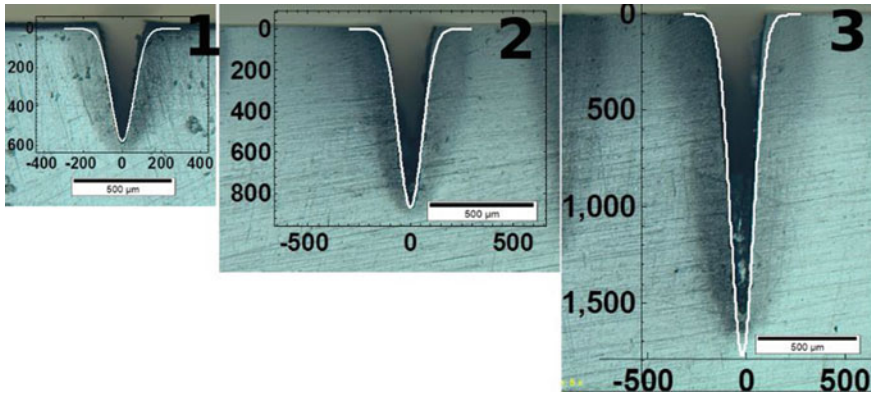


Fig. 10 Actual and predicted microchannel profiles

6 Conclusions

CO₂ laser has been used successfully to create microchannels on PMMA. The etched microchannels are clean with negligible amount of burrs around the channel. The developed model utilizes fundamental physical aspects of thermodynamics. The material properties of PMMA have been determined utilizing spectroscopy and simultaneous TGA/DSC. The developed model presents an excellent agreement between actual and predicted channel profiles. The successful modeling requires the accurate values of material properties. The developed model can be used directly to predict channel depth and profiles. The model has been found to predict the dimensions accurately over a large zone of dimensions. Computational approaches, though more accurate, consume time in order to predict the microchannel profiles and depth. Energy based analysis presents an easy solution for CO₂ laser machining of PMMA.

Acknowledgments The authors gratefully acknowledge the financial support from Department of Science and technology (DST), Govt. of India for providing INSPIRE fellowship to one of the author for carrying out this research.

References

- Castaño-Álvarez, M., Pozo Ayuso, D. F., Garcia Granda, M., Fernández-Abedul, M. T., Rodriguez Garcia, J., & Costa-Garcia, A. (2008). Critical points in the fabrication of microfluidic devices on glass substrates. *Sensors and Actuators B: Chemical*, 130, 436–448.
- Dahotre, N. B., & Harimkar, S. P. (2007). *Laser Fabrication and Machining of Materials* (1st ed.). Springer, London.
- Helebrant, A., Buerhop, C., & Weissmann, R. (1993). Mathematical modelling of temperature distribution during CO₂ laser irradiation of glass. *Glass Technology*, 34(4), 154–158.

- Iliescu, C., Taylor, H., Avram, M., Miao, J., & Franssila, S. (2012). A practical guide for the fabrication of microfluidic devices using glass and silicon. *Biomicrofluidics*, 6(1), 016505.
- Julia, J. E., Aboites, V., & Casillas, M. A. (1998). CO₂ laser interaction with biological tissue. *Instrumentation and Development*, 3(10).
- Klank, H., Kutter, J. P., & Geschke, O. (2002). CO₂-laser micromachining and back-end processing for rapid production of PMMA-based microfluidic systems. *Lab on a Chip*, 2(4), 242–246.
- Madic, M., Radovanovic, M., & Nedic, B. (2012). Correlation between surface roughness characteristics in CO₂ laser cutting of mild steel. *Tribology in Industry*, 34(4), 232–238.
- Malek, C. G. K. (2006). Laser processing for bio-microfluidics applications (part ii). *Analytical and Bioanalytical Chemistry*, 385(8), 1362–1369.
- Powell, J. (1998). *CO₂ laser cutting* (2nd ed.). London: Springer.
- Prakash, S., & Kumar, S. (2014). Fabrication of microchannels: A review. In: *Proceedings of the Institution of Mechanical Engineers, Part B: Journal of Engineering Manufacture*. doi:10.1177/0954405414535581.
- Prakash, S., Acherjee, B., Kuar, A. S., & Mitra, S. (2013). An experimental investigation on ND: YAG laser microchanneling on polymethyl methacrylate submerged in water. *Proceedings of the Institution of Mechanical Engineers, Part B: Journal of Engineering Manufacture*, 227(4), 508–519.
- Qi, H., Chen, T., Yao, L., & Zuo, T. (2009). Micromachining of microchannel on the polycarbonate substrate with CO₂ laser direct writing ablation. *Optics and Lasers in Engineering*, 47(5), 594–598.
- Radice, J. J., Joyce, P., Tresansky, A., & Watkins, R. (2012). A comsol model of damage evolution due to high energy laser irradiation of partially absorptive materials. In: *Excerpts from the Proceedings of the 2012 COMSOL Conference in Boston*.
- Russom, A., Gupta, A. K., Nagrath, S., Carlo, D. D., Edd, J. F., & Toner, M. (2009). Differential inertial focusing of particles in curved low-aspect-ratio microchannels. *New Journal of Physics*, 11(7), 075025.
- Shulepov, M. A., Bulgakova, N. M., Zakharov, L. A., Panchenko, A. N., & Telminov, A. E. (2010). CO₂ laser ablation of poly (methyl methacrylate) and polyimide: Experiment and theory. In: *Proceedings of the 10th International Conference on Modification of Materials with Particle Beams and Plasma Flow* (pp. 132–135).
- Snakenborg, D., Klank, H., & Kutter, J. P. (2004). Microstructure fabrication with a CO₂ laser system. *Journal of Micromechanics and Microengineering*, 14(2), 182.
- Xiang, H., Fu, J., & Chen, Z. (2006). 3D finite element modeling of laser machining PMMA. In: *1st IEEE International Conference on Nano/Micro Engineered and Molecular Systems, 2006, NEMS'06* (pp.942–946).
- Yuan, D., & Das, S. (2007). Experimental and theoretical analysis of direct-write laser micromachining of polymethyl methacrylate by CO₂ laser ablation. *Journal of Applied Physics*, 101(2), 024901.
- Zhou, B. H., & Mahdavian, S. M. (2004). Experimental and theoretical analyses of cutting nonmetallic materials by low power CO₂-laser. *Journal of Materials Processing Technology*, 146(2), 188–192.